ԵՐԵՎԱՆԻ ՊԵՏԱԿԱՆ ՀԱՄԱԼՍԱՐԱՆ

ՀԱՅԱՍՏԱՆԻ ՀԱՆՐԱՊԵՏՈՒԹՅԱՆ ԳԻՏՈՒԹՅՈՒՆՆԵՐԻ
ԱԶԳԱՅԻՆ ԱԿԱԴԵՄԻԱ

ԿԻՍԱՀԱՂՈՐԴՉԱՅԻՆ ՄԻԿՐՈ- ԵՎ ՆԱՆՈԷԼԵԿՏՐՈՆԻԿԱ

ՏԱՍՆԱՄԵԿԵՐՈՐԴ ՄԻՋԱԶԳԱՅԻՆ ԳԻՏԱԺՈՂՈՎԻ ՆՅՈՒԹԵՐ
ԵՐԵՎԱՆ, 23-25 ՀՈՒՆԻՍ

SEMICONDUCTOR MICRO- AND NANOELECTRONICS

PROCEEDINGS OF THE ELEVENTH INTERNATIONAL CONFERENCE
YEREVAN, ARMENIA, JUNE 23-25

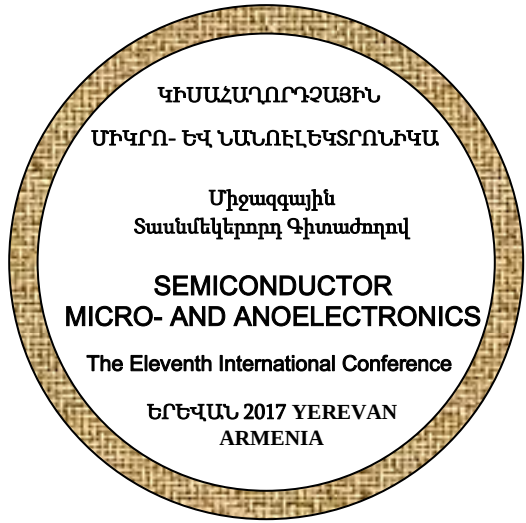

Երևան

ԵՊՀ հրատարակչություն

2017

BIOCHEMICAL SENSORS

BASED ON SILICON NANORIBBON FETs
Part 1: Samples Fabrication, CVCs, pH-sensitivity

F. Gasparyan[1,2], I. Zadorozhnyi[2], H. Khondkaryan[1], A. Arakelyan[1], S. Vitusevich[2]

[1]Yerevan State University, 1 Alex Manoogian St., 0025, Yerevan Armenia
[2]Peter Grünberg Institute (PGI-8), Forschungszentrum Jülich, 52425 Jülich, Germany

1. Introduction

Over the past decade, nanosized silicon structures have been under intensive study due to their promising electrical, optical, chemical, thermal and mechanical properties. Compared to larger structures, nanoscale field-effect transistors (FET) are capable of measuring electrical, optical and other types of very small signals due to increased surface-to-volume ratio of the sample. The small sizes of nanostructures make them ideal for sensing of small sample volumes with low analyte concentrations. For example, in the field of medical diagnostics an incredibly small volume structures aiming the integration of 1D nanostructure such as carbon nanotubes, metallic and semiconducting nanowires (NW) and nanoribbons (NR) can be utilized for a variety of applications. Among the mentioned structures, silicon nanoribbon (NR) and nanowire (NW) field –effect transistor (FET) structures open prospects for label-free, real-time and high-sensitive detection of biomolecules using affinity-based detection [1]. The sensitivity of different NR dimensions was studied in [1]. It was illustrated that the new integrated NR sensor with reference NR can be utilized for real-time error monitoring during pH-sensing [1]. New features and functions are continuously added to the electronic devices, i.e. health monitoring mobile systems and wearable devices. Despite the success of such personal health monitoring systems [2], the next generation of wearable devices is expected to include also a portable "lab-on-a chip" – set of medical biosensors which can be used for the detection and diagnosis of various medical conditions[3,4]. In order to be able to monitor and detect the early stages of disease, the size of the sensor transducer has to be comparable with the biological markers. Therefore biosensors based on NWs and NRs have to be capable to monitor the biological events that occur at very small dimensions. Another important area of application is optoelectronic, where the interaction of different wavelengths of light with nanostructures may be used for future optical device applications. Sub-wavelength diameters and proximity effects may lead to interesting optical properties such as low reflectance and thus high absorption. Investigations of SiNW optical absorption have shown the strong size-dependent effects [5,6]. Studies of the broadband optical absorption showed increased total optical adsorption spectra for SiNW samples [7]. SiNWs lead to a significant reduction of the reflectance compared to the solid silicon films [7,8]. Optical absorption increases while the wavelength decreases. It should be noted that, unlike the bulk material, nanosized Si structures may be direct band gap semiconductors. Such properties make them excellent choice for optical applications [6,9-12]. On the other hand, the size scaling brings to the increased band gap [9]. This may result in a successful shift of the absorption spectra to short wavelengths [6,12]. With size decrease the limitations regarding current and voltage have also be considered. For devices operating at weak signal levels internal noise plays crucial role [13-15]. It determines one of the most important parameters of sensors - signal-to-noise ratio (SNR). As it is shown for double gated SiNW sensors pH-sensitivity increases with the liquid gate voltage and SNR has higher value ($\sim 10^5$) [6,12]. The nanoribbon approach opens up for large scale CMOS fabrication of highly sensitive biomolecule chips for potential use in medicine and biotechnology [16].

The present work is devoted to the study of silicon nanoribbons-based FETs and consists of two parts. In the first part, the sample fabrication technology, and chip characterization - their dark and light current-

voltage characteristics (CVC) and pH-sensitivity are presented. In the second part low-frequency noise studies, size-dependent effects of the pH-sensitivity and source-drain currents are described. We demonstrate that silicon nanoribbons, in this case, a thin sheet of silicon on an oxidized silicon substrate, can have high pH-sensitivity fairly close to the Nernst limit.

2. Samples and experimental technique

Silicon nanoribbon (NR) structures were fabricated on the basis of silicon-on-insulator (SOI) wafers purchased from SOITEC. The process starts from the thermal oxidation to form 20 nm thick silicon oxide hard masks. The active silicon layer thickness is 50 nm. NRs of various geometries are then patterned in hard mask using optical lithography with following reactive ion etching process step. The pattern is transferred into silicon using wet chemical etching in the tetramethylammonium hydroxide (TMAH) solution. Gate dielectric which also serves as a channel protection from liquid environment was thermally grown 8nm thick silicon oxide. The NR channel was almost undoped Si NR channel with hole concentration of 10^{15} cm^{-3}. Source and drain contacts were highly doped to form good ohmic contact. For the connection to electronics Aluminum contacts were patterned using a lift-off process. Finally chips were passivated with polyimide layer to protect metal feed lines from liquid environment.

3. CVCs and pH-sensitivity

Figures 2 and 3 show source-drain current-voltage characteristics (CVCs) of samples under study measured at back gate voltages of -1V and -5 V, correspondingly. Characteristics measured in the dark conditions as well as under specific power illuminations of 0.85 W/cm^2 and 1.6 W/cm^2 at room temperature. Light excitation is performed using incandescent lamps located at a distance of 15 cm from the sensor. The CVC dependencies demonstrate typical behavior which is similar to the solid silicon FET CVCs [17] since the samples under investigation have relatively large dimensions of $l \times w \times t = (2 \div 10) \times 10 \times 0.05$ μm (l, w and t are the channel length, width and thickness, correspondingly). Presented in Figs. 2-3 CVCs can be described as:

$$I_{ds} = I_{ds,d} + I_{ds,ph}, \quad (1)$$

where $I_{ds,d}$ and $I_{ds,ph}$ are the dark and photo current components. Dark current can be described by the well-known expression of CVC for the n-channel MOSFETs for $V_{ds} \le V_{gs} - V_{th}$ [17]:

$$I_{ds,d} = \frac{w\mu_n C_{ox}}{l}\left(V_{gs} - V_{th} - \frac{V_{ds}}{2}\right)V_{ds}. \quad (2)$$

Here $C_{ox} = \varepsilon_{ox}/t_{ox}$ is the oxide layer capacitance per unit area, ε_{ox} and t_{ox} are the permittivity and thickness of the gate oxide layer, V_{gs} and V_{th} are gate-source and threshold voltages.

In the approximation the Eq. (2) can be applied for the n-channel. We can present photo current as following:

$$I_{ds,ph} = A_{ch} e \mu_p \Delta p \frac{V_{ds}}{l} = A_{ch} e \mu_p \eta \alpha \tau_p \frac{W}{h\nu} \frac{V_{ds}}{l}. \quad (3)$$

Here $A_{ch} = wt$ is the current channel cross-section area, Δp the concentration of excess photo carriers (holes), α the illumination absorption coefficient, η the quantum yield, τ_p the hole's life time, $h\nu$ the photon energy, W the illumination specific power in [W/cm^2].

In Eq. (3) we assumed that the electric field strength is uniformly distributed along the channel length and the value of A_{ch} slightly varies along the length of the channel. It should be noted that this assumption is valid in the main part of the channel, which is far from source and drain contacts.

At low voltages V_{ds}, the source-drain current I_{ds} grows approximately linearly with voltage and tends to saturation at high voltages. The magnitude of the I_{ds} increases, with increasing light specific power. Figs. 4-5 shows CVCs of the investigated device at the several front gate voltages (V_{FG} = -1 V, -5 V) measured in an aqueous solution with pH= 6.2, 7 and 8.3. We can see that increasing of the pH-value results in the increase of the channel current, I_{ds}. This is in a good agreement with model of the solution contact with the

oxide layer surface, then on the oxide/solution interface caused hydroxyl groups SiOH. Concentration and behavior of those hydroxyl groups depends on value of the pH. The case when the surface is not charged is called zero charge point. For the SiO_2 dielectric layer the point is reached at $\mathbf{pH_0 = 2.2}$. At the pH-values lower $\mathbf{pH_0}$ the oxide surface is charged positively, at higher values of the pH, oxide surface is charged negatively. In the case of buffer solution with pH = 7 silicon oxide surface charge will be charged negatively, correspondingly Therefore, at the applied negative gate potential the absolute value of the negative charge on the surface oxide increases. As a result, the concentration of the majority carriers in the current channel (holes in p-Si) and therefore current increases.

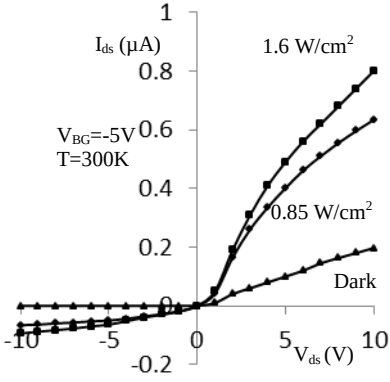

Fig. 2. Output CVCs of SiNR FET sample with length $l = 10$ μm, measured in the dark and at excitation by the light specific power 0.85 W/cm^2 and 1.6 W/cm^2 at V_{BG} = -1V, T = 300 K.

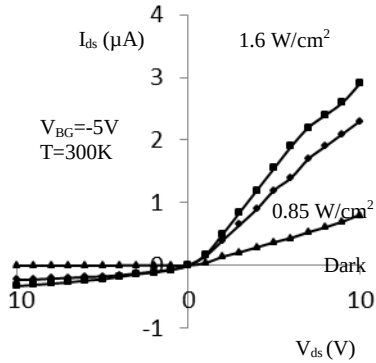

Fig. 3. Output CVCs of SiNR FET sample with length $l = 10$ μm, measured in the dark and with excitation by the light specific power 0.85 W/cm^2 and 1.6 W/cm^2 at V_{BG} = -5 V, T = 300 K.

Figures 4 and 5 show the CVCs of the SiNR structures working in biochemical sensing mode. In [18] pH-sensitivity of the biochemical sensors was introduced as

$$R_{pH} = \frac{R_{ch}\Delta I_{ds}}{\Delta pH}. \quad (4)$$

Here ΔI_{ds} and ΔpH are the elementary changes in I_{ds} and pH. Note that pH-sensitivity is the measurable value. In the solution medium with the increased pH value the source-drain current increases. This allows the registration of the pH variation in any bio liquids with high accuracy. For example, for $V_{BG} = -5$ V at the V_{ds}=5 V the sensitivity is equal to R_{pH}≈56.4 mV/pH. At the $V_{BG} = -10$ V the pH-sensitivity grows up to 59.3 mV/pH and approaches the Nernst limit 59.5 mV/pH [19]. The pH-sensitivity grows with increase of back-gate voltage. For example from Figs. 4 and 5 at the V_{ds}=8 V we obtained the ratio $(R_{pH})_{V_{BG}=-5\,V}/(R)_{V_{BG}=-1\,V} \approx 5.17$, i.e. approximately 5 times improved sensitivity.

4. Conclusion

Silicon nanoribbon FET biochemical sensors of various lengths were fabricated. Their static dark and light-induced CVCs as well as the behavior of these sensors in an aqueous solution with different values of pH are investigated. The static dark CVC dependencies show that the characteristics correspond to high quality silicon FET CVCs. With increasing light intensity, the source-drain current grows because of the increase in

the conduction of the current channel. The pH-sensitivity increases with the increasing of the back gate voltage and approaches to the Nernst limit of 59.5 mV/pH.

Acknowledgments: This work was supported by the SCS MES of Armenia in the framework of research Project No. 15T-1C 279. F. Gasparyan greatly appreciates the support from the German Academic Exchange Service (DAAD) in the form of a research grant. The authors would like to acknowledge for the Innovation Award of RWTH Aachen University in the framework of RWTH transparent 2016.

The list of used literature is given in the second part of this work.

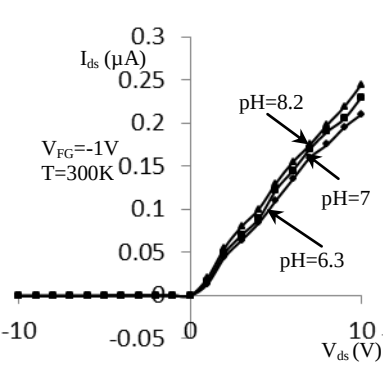

Fig. 4. Output CVCs of SiNR FET with length $l = 10\ \mu m$, measured in the dark and pH concentrations 6.3, 7, 8.2 at V_{FG} =-1 V, T =300 K.

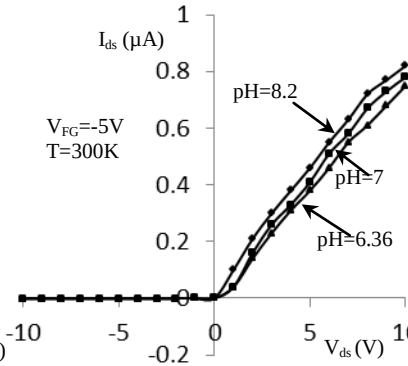

Fig. 5. Output CVCs of SiNR FET with length $l = 10\ \mu m$, measured in the dark and pH concentrations 6.3, 7, 8.2 at V_{FG} =-5 V, T =300 K.